ORIGINAL ARTICLE

Spontaneous formation of interdigitated array pattern in wrinkled gold films deposited on poly(dimethylsiloxane) elastomer

Masashi Watanabe, Ryou Hatano and Chiho Koizumi

In this study, we attempted to produce a gold coating on a glass slide with an interdigitated array (IDA) pattern through a series of processes including spontaneous pattern formation as a key step instead of using photolithographic micromachining processes. In the first step, a gold film was formed by sputter deposition onto a strip of poly(dimethylsiloxane) (PDMS) elastomer. As part of the deposition process, the strip was heated because of the excess kinetic energy of the sputtered atoms. As the strip cooled to room temperature after the deposition, it thermally shrunk, causing the gold film to wrinkle because of buckling instability. Most of the wrinkles were oriented in a direction perpendicular to the lengthwise direction of the strip. In the second step, a glass strip that was narrower than the PDMS strip was placed on the PDMS strip. Sputter deposition of gold was repeated, resulting in the formation of wrinkles with an IDA pattern. Finally, this pattern was replicated on an elastomeric stamp surface that was then used for patterning a gold coating on a glass slide using microcontact printing techniques.
Polymer Journal (2015) **47**, 320–327; doi:10.1038/pj.2014.116; published online 7 January 2015

INTRODUCTION

An interdigitated array (IDA) electrode typically consists of two comb-shaped electrodes that are arranged in an interlocking but separated manner. Although studies on surface elastic waves by White and Voltmer[1] and on electrochemical analyses by Sanderson and Anderson[2] are representative early studies using IDA electrodes, current applications of IDA electrodes cover an extremely wide range, from biosensors to electronics.

In biosensors, IDA electrodes are used for immunoassays,[3] detection of bacteria[4] and analyses of biomolecules such as proteins[5] and DNA.[6] Various chemicals can also be detected, which include endocrine disrupters,[7] herbicides[8] and toxic gases, such as ammonia,[9] formaldehyde[10] and nitrogen dioxide.[11] As other types of sensors using IDA electrodes, optical sensors using photoconductors[12] and humidity sensors are reported.[13]

In electronics, IDA electrodes are more accurately called interdigital transducers. Surface acoustic wave (self-assembled monolayer (SAM)) filters using interdigital transducers are key components for mobile terminals such as cell phones.[14] In microelectromechanical systems, surface acoustic wave motors[15] and electrostatic comb-drive actuators are reported.[16]

In chemical engineering at small scale such as lab-on-a-chip technologies, various unit operations are performed using surface acoustic waves generated by interdigital transducers, which include mixing,[17] extraction,[18] heating[19] and manipulation of droplets.[20]

As other examples of applications, IDA electrodes are employed for ordering small objects such as cells,[21] polymer particles,[22] metallic

nanowires[23] and carbon nanotubes.[24] They can also be used for electroorganic syntheses.[25] Thus, IDA electrodes are versatile components in various fields.

In sensing applications, IDA electrodes with a miniature size, that is, IDA microelectrodes, have various advantages because of their size and unique shape. Although there are many sensing methods, we describe capacitive and electrochemical methods, as follows.

In capacitive sensors, the change in the capacitance between two metal electrodes is measured.[26] When analyte molecules react with probe molecules immobilized between the electrodes, the reaction is detected as a change in capacitance. As can be seen from the fact that the capacitance of a plate capacitor is proportional to the electrode area and is inversely proportional to the distance between the electrodes, an IDA microelectrode, which has a large effective electrode area and a small electrode gap, is advantageous for improving sensitivity.

As described early in the introduction, an IDA microelectrode consists of two comb-like electrodes. In electrochemical sensors, one of the electrodes (generator electrode) oxidizes an analyte of interest and the other (collector electrode) detects the oxidized species and simultaneously reduces it. The reduced species, which is the same as the original analyte, diffuses back to the generator electrode. Thus, a redox cycle forms, which enhances the current so that the sensitivity of the sensor is significantly improved.[27] In addition, when the IDA electrode is an array of narrow-band electrodes, a steady-state current can rapidly be achieved, which improves signal-to-noise ratio.[2]

Thus, an advantage of IDA microelectrodes is the improvement of the sensitivity of chemical or biochemical sensors.

Photolithographic micromachining techniques are usually used for fabricating IDA microelectrodes.[28] However, there are some reports in the literature of other fabrication methods that use various printing
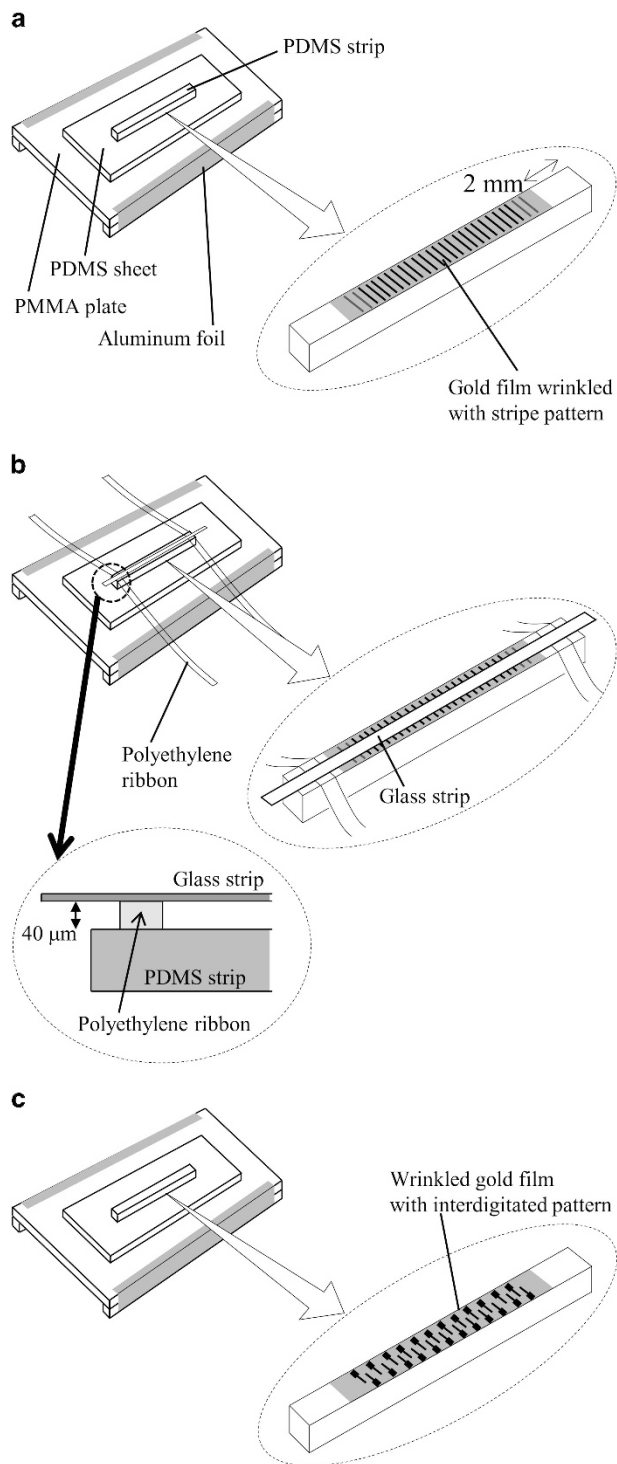
Figure 1 Schematic diagram of procedure to form wrinkled gold films with interdigitated array pattern. (**a**, **b**) First and second deposition of gold. (**c**) Finally obtained wrinkles with interdigitated pattern. PDMS, poly (dimethylsiloxane); PMMA, poly(methyl methacrylate).

techniques, such as inkjet printing,[29] laser printing,[30] screen printing,[31] nanotransfer printing[32] and direct ink writing.[33] Although photolithographic techniques can produce IDA microelectrodes with a precisely controlled shape, they usually require expensive equipment and multiple time-consuming processes. Stencils for screen printing and stamps for nanotransfer printing are also fabricated using photolithographic techniques. In contrast, the fabrication process using inkjet printing is simple and cost-effective because it does not include photolithographic processes. However, the resolution of inkjet printing (usually more than 30 μm) seems to be insufficient to fabricate IDA microelectrodes.[34] Although the resolution of direct ink writing (several μm) is smaller than that of normal inkjet printing, specialized, sophisticated equipment is required.

In this study, we propose a novel method for fabricating IDA microelectrodes. In this method, a spontaneously formed IDA pattern of wrinkles of thin, gold films is used for fabricating stamps for microcontact printing. Such wrinkle formation is based on a phenomenon called buckling instability[35] and microcontact printing is one of the well-known techniques, called soft lithography.[36]

Buckling instability has attracted much attention as a strategy for controlling surface topography on micro- and nanometer scales since 1998 when Bowden et al. reported a simple method to form micro-wrinkles of thin gold films on top of thick poly(dimethylsiloxane) (PDMS) elastomers.[37] When compressive stress in a stiff, thin film on a soft, thick substrate exceeds a certain critical value, regular wrinkles form owing to buckling instability.[35] As material for the stiff, thin films, gold,[37,38] platinum[39] and aluminum[40] can be employed. Silica-like thin films that are formed on the surface of PDMS through exposure to oxygen plasma,[41] ultraviolet light[42,43] or acidic solution[44–47] are also used. For a soft, thick substrate, PDMS is one of the commonly used materials, probably because a microscopically flat surface is easily obtained by casting a liquid precursor of PDMS on a plate followed by vulcanizing the precursor. Various methods to generate compressive stress in stiff, thin films are known. For example, thermal shrinkage,[37] mechanical force[48] or swelling with appropriate solvents[49] is utilized.

Wrinkles formed because of buckling instability exhibit various patterns as well as simple stripes.[48] Patterns reported so far include herringbone,[50] spoke,[51] target[51] and checkerboard patterns.[43,52] However, to the best of our knowledge, IDA patterns have not yet been reported, whereas IDA microelectrodes are widely used for various applications, as described above.

In particular, some applications of chemical and biochemical sensors, such as point-of-care testing toward hazardous agent detection, food inspection and clinical diagnostics, must be disposable.[53–55] We believe that inexpensive, disposable, single-use IDA microelectrodes are useful for these applications for the following reason. An electrode that is used repeatedly to analyze multiple samples must be sufficiently cleaned before each use in order to prevent cross-contamination.[56] However, complete cleaning is difficult in analytical applications, such as point-of-care testing for clinical diagnostics and on-site environmental analysis, because cleaning facilities are often unavailable. Therefore, we believe that there is a demand for relatively inexpensive IDA microelectrodes that are disposable. Presently, commercially available IDA microelectrodes are mainly produced using photolithographic micromachining techniques, causing these electrodes to not be sufficiently low-cost, and therefore unsuitable for disposable use. In this study, we attempted to do away with costly photolithographic processes to produce IDA electrodes. Instead, we used cost-effective, spontaneous formation of IDA patterns of wrinkles. Although this attempt has not yet been satisfactorily

accomplished, we were able to obtain some promising results that suggest the possibility of developing inexpensive IDA microelectrodes.

EXPERIMENTAL PROCEDURE

Materials

A precursor of the PDMS elastomer (KE-103), a curing agent (CAT-103) and a silicone oil (KF-96H-10000CS) were purchased from Shin-Etsu Chemical Co., Ltd. (Tokyo, Japan). Thin glass slides (18×18 mm^2, ca 0.15 mm thick) were acquired from Matsunami Glass Ind., Ltd. (Osaka, Japan). Thiourea and iron (III) sulfate were obtained from Wako Pure Chemical Industries, Ltd. (Osaka, Japan). Temperature-indicating labels were supplied from NiGK Corporation (Kawagoe, Japan).

Preparation of PDMS elastomer

The precursor of the PDMS elastomer (KE-103) and the curing agent (CAT-103) were mixed in a weight ratio of 100:5 and degassed under vacuum. The mixture was cast on a poly(methyl methacrylate) plate. Vulcanization of the mixture proceeded at room temperature for 3 days. The obtained 1.2-mm-thick PDMS sheet was then cut into a strip of 0.85 mm wide and 14 mm long. Onto this PDMS strip, gold was deposited, as described in the next section.

Deposition of gold onto PDMS strips

A small amount of silicone oil was applied to a poly(methyl methacrylate) plate (18×30 mm^2, 2 mm thick) and then a piece of the PDMS sheet (9×22 mm^2, 1.2 mm thick) was placed on the plate (Figure 1a). After a minute, quantity of silicone oil was applied to the PDMS sheet, a PDMS strip (0.85×14 mm^2, 1.2 mm thick) was carefully placed in the center of the PDMS sheet. The PDMS strip was then heated at 100 °C for 1 h to remove strains in the PDMS sample.

Sputter deposition of the gold was carried out using a DC sputtering coater (IB-3, Eiko Engineering, Co., Ltd., Hitachinaka, Japan) at a deposition rate of 1.8 nm min^{-1}. The potential difference and current between the gold target and the sample stage were controlled to be 980 V and 3.0 mA, respectively. The deposition rate was estimated based on the data that the manufacturer of the coater provided.

Sputter deposition was repeated twice. During the first deposition, both ends of the PDMS strip were covered with polyethylene films of 2 mm wide as masks so as to not deposit gold on these parts (see Figure 1a, circled magnified figure).

a

Gold film

Mold

PDMS strip

b

Negative replica

Gold film

c

Gold film

Positive replica

d

Stamp

Figure 2 Schematic diagram of procedure to fabricate an elastomeric stamp by replicating the pattern of a wrinkled gold film. PDMS, poly (dimethylsiloxane).

After the deposition, a 40-μm-thick polyethylene ribbon was placed at each end of the PDMS strip and a glass strip (ca 0.50 mm wide, 18 mm long and 0.15 mm thick) was put on the ribbons (Figure 1b). The position of the strip was carefully adjusted to the center axis of the PDMS strip by observing the glass and PDMS strips using a light microscope. Finally, the second deposition was performed. A wrinkled gold film with IDA pattern was formed on the surface of the PDMS strip (Figure 1c).

Microcontact printing

Elastomeric stamps were fabricated by replicating a mold consisting of the PDMS strip covered with the wrinkled gold film. First, a mixture of the PDMS precursor (KE-103) and the curing agent (CAT-103) in a weight ratio of 100:5 was cast on the mold (Figure 2a), followed by curing at 45 °C for 1 h. The vulcanized PDMS elastomer, that is, the negative replica (Figure 2b) was easily separated from the mold because the gold film prevented the replica from sticking to the mold. During this separation, the gold film transferred from the mold to the negative replica. Next, the mixture was cast on the negative replica and cured at 45 °C to obtain a positive replica (Figure 2c). In this replication, the positive replica was also easily separated from the negative replica. The positive replica was additionally cured at 100 °C for 1 h. Finally, the residual gold film on the positive replica was removed by soaking it in an etching solution[57] (an aqueous mixture of 0.25 M thiourea, 0.25 M iron (III) sulfate and 0.038 M sulfuric acid; Figure 2d). The obtained replica was used as a stamp in the next step.

The stamp was soaked in an ethanol solution of 1-eicosanethiol (1.5 mM) for a few minutes, followed by drying in air.[36] A glass slide that was pretreated with 1,1,1,3,3,3-hexamethyldisilazane was coated with gold using sputter deposition. The stamp was brought into contact with the slide for ca 0.5 s. The slide was then immersed in the previously described etching solution at room temperature and rinsed with water. The resulting gold pattern was observed using a light microscope.

Examination of the surface of the wrinkled gold film

The surface was observed using a light microscope (MELUX-2-1L, Kyowa Optical Co., Ltd., Kanagawa, Japan). The surface profile was measured using a laser surface profiler (LT-9000, Keyence Corporation, Osaka, Japan) that scanned the surface linearly.

Measurement of Young's modulus and coefficient of thermal expansion of PDMS elastomer

Young's modulus and the coefficient of linear thermal expansion of the PDMS elastomer were measured using a thermomechanical analyzer (TMA/SS6100, Seiko Instruments, Chiba, Japan) in tensile mode.

RESULTS AND DISCUSSION

Control of wrinkle orientation

Gold was deposited onto a PDMS strip using a DC sputtering technique for 35 min at a deposition rate of 1.8 nm min^{-1}. As shown in Figure 3, a well-ordered stripe pattern was observed on the top surface of the PDMS strip using a light microscope. The sinusoidal profile measured by a surface profiler indicated that the stripe pattern had substantially a regularly wrinkled surface topography (Figure 4). The white and ocher-colored parts of the microscope image (Figure 3) indicate the valleys (that is, concave parts) and peaks (that is, convex parts) of the wrinkles, respectively. The wavelength, λ, and the peak-to-valley amplitude, A, of the wrinkles were 37 μm and 1.1 μm, respectively (Figure 5). In this section, we will first discuss the cause of the wrinkling and then the mechanism of the orientation of the wrinkles.

The cause of the wrinkling has already been explained by many groups describing a force balance[35] or an energy balance[58] between the bending of a stiff, thin film and the stretching of a soft, thick substrate (Figure 5). Compressive stress exceeding some critical value induces wrinkling of the surface. This phenomenon is called buckling
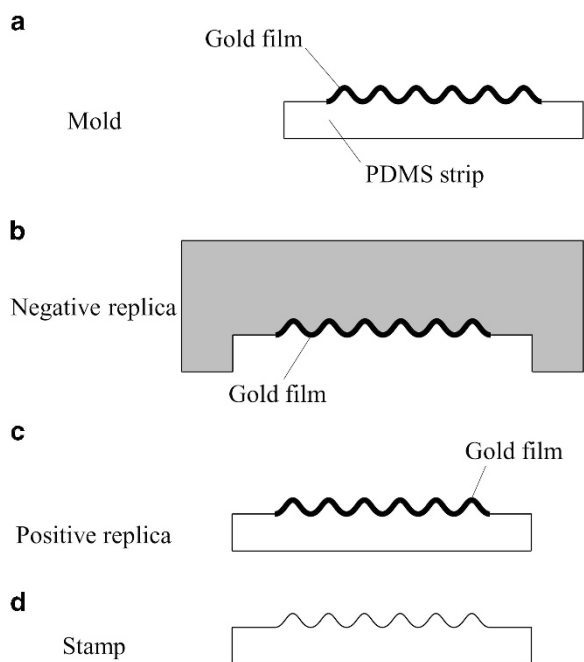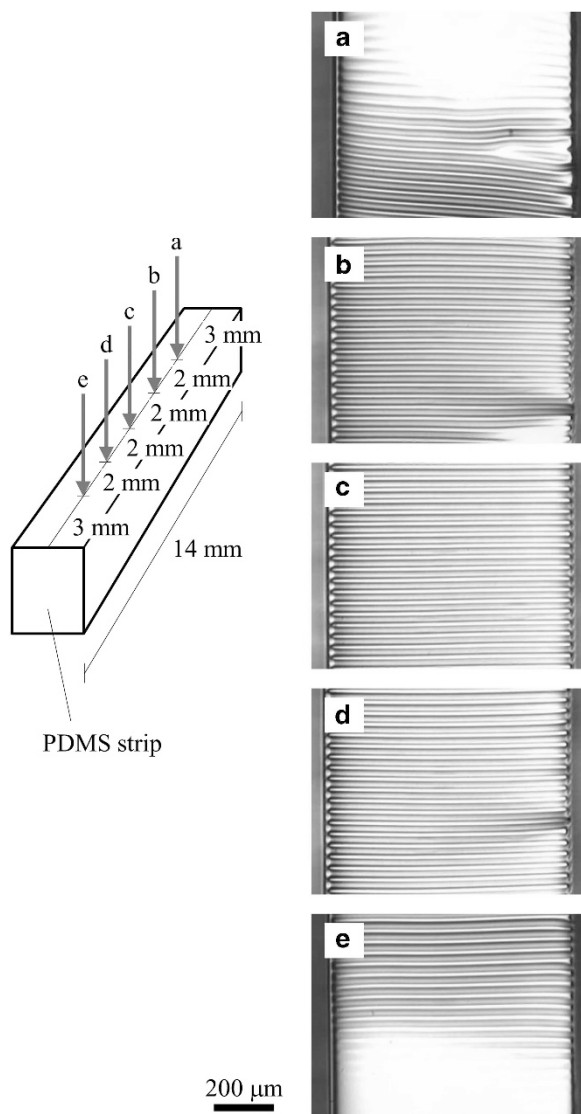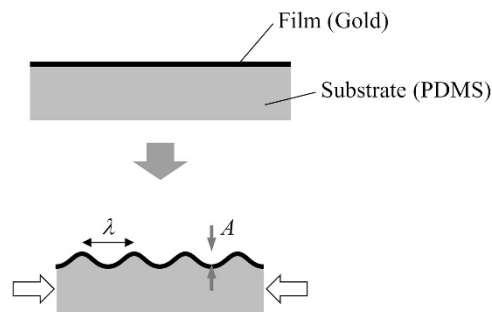
Figure 3 Light microscope images of gold film obtained using sputter deposition. The left diagram illustrates the observation position for each image (**a**–**e**). PDMS, poly(dimethylsiloxane). A full color version of this figure is available at *Polymer Journal* online.
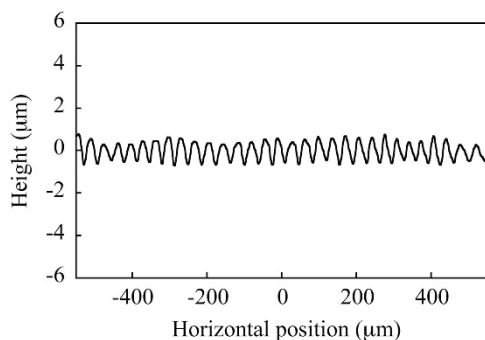

Figure 4 Profile of wrinkled gold film deposited onto poly(dimethylsiloxane) strip.

instability. In this study, the stiff, thin film and the soft, thick substrate corresponded to the deposited gold (thickness $h_f = 64$ nm, Young's modulus $E_f = 80$ GPa,[59] Poisson's ratio $\nu_f = 0.42$[59]) and PDMS
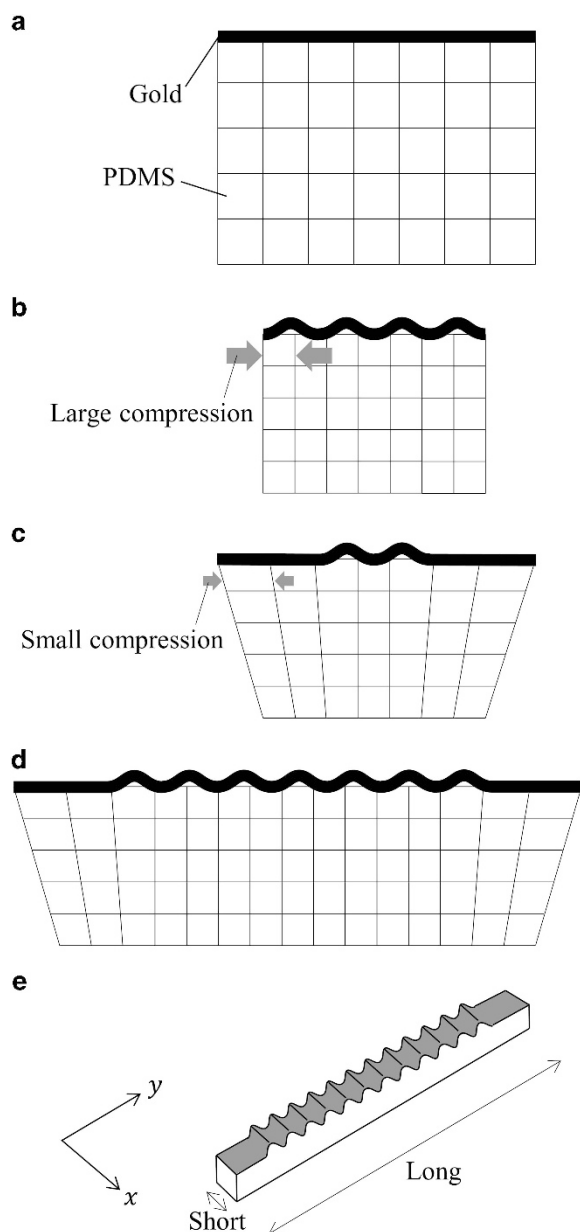

Figure 5 Schematic diagram of mechanism of wrinkling of gold film on top of poly(dimethylsiloxane) (PDMS) substrate.
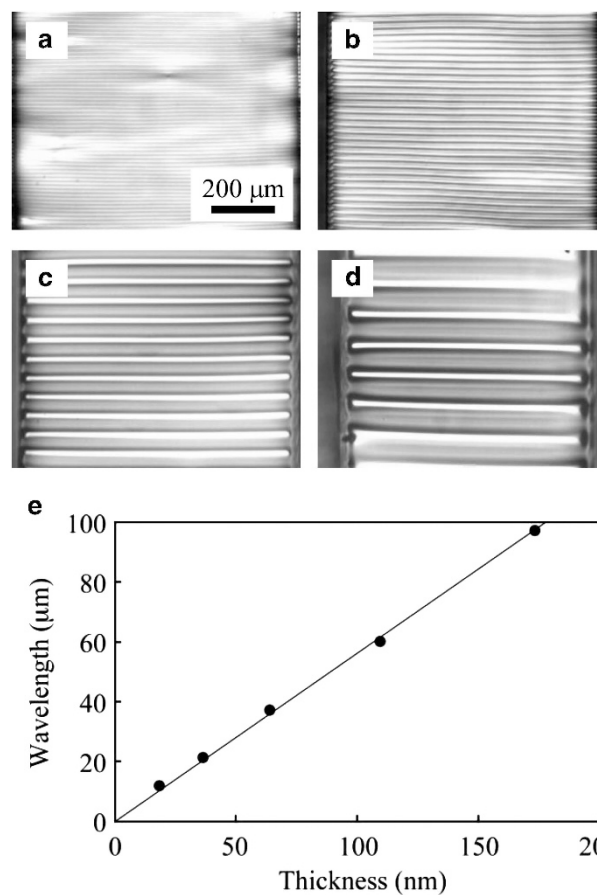
Figure 6 Light microscope images of wrinkled gold films of (**a**) 18, (**b**) 37, (**c**) 110 and (**d**) 173 nm in thickness. (**e**) Relationship between thickness of gold film and wrinkle wavelength. A full color version of this figure is available at *Polymer Journal* online.

(Young's modulus $E_s = 0.89$ MPa, Poisson's ratio $\nu_s = 0.48$[37]), respectively. Compressive stress originated from the thermal shrinkage of the PDMS because the PDMS strip was heated because of the excess kinetic energy of the sputtered atoms and then cooled to room temperature after the deposition. The temperature of the surface of the PDMS strip during sputter deposition was around 80 °C, which was roughly measured using a temperature-indicating label. The coefficient of linear thermal expansion of the PDMS employed in this study was 3.1×10^{-4} K^{-1}. From these results, the strain induced by the thermal shrinkage was estimated to be around 1.9%.

a

Gold

PDMS

b

Large compression

c

Small compression

d


e

y

x

Long

Short

Figure 7 Schematic diagrams of a possible mechanism controlling the orientation of wrinkles. PDMS, poly(dimethylsiloxane).

It is known that the wrinkle wavelength, λ, theoretically follows the equation.[35]

$$\lambda = 2\pi h_f \left\{ \frac{(1-v_s^2)E_f}{3(1-v_f^2)E_s} \right\}^{\frac{1}{3}} \quad (1)$$

The wavelength calculated using this equation was 12 µm, whereas that measured based on the light microscope image (Figure 3) was 37 µm. These values were of the same order, although the measured one was around three times greater than the calculated one. A similar difference was also reported by Bowden *et al.*[37] They attributed the difference to the thermal crosslinking of PDMS at the surface during deposition of the gold. Recently, such modification of PDMS surfaces was reported using X-ray photoelectron spectroscopy by Casper *et al.*[60] Figure 6 shows the relationship between the thickness of the gold film and the wrinkle wavelength. The wavelength, λ, was proportional to the thickness, h_f, which was qualitatively consistent with Equation 1.

λ

2λ

2λ

Array of wrinkles
with wavelength of λ
(Center part)

(Side parts)
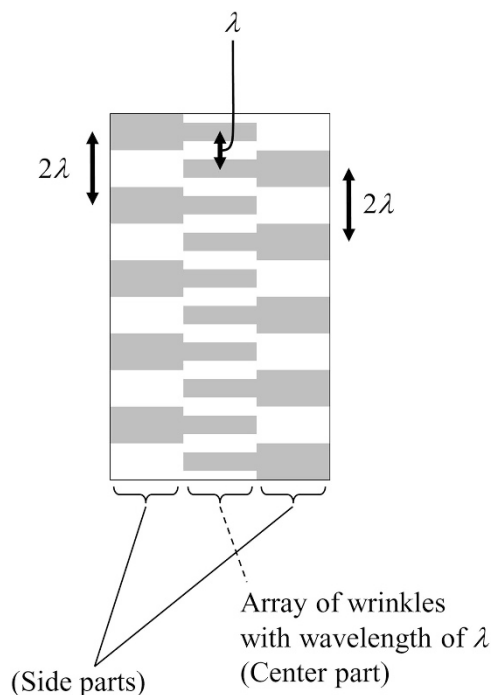
Figure 8 Schematic diagram of a method to create an interdigitated array pattern.

Next, we discuss a possible mechanism controlling the orientation of the wrinkles. During the sputter deposition, the PDMS elastomer is heated and thus thermally expanded (Figure 7a). When the PDMS elastomer is cooled to room temperature, it shrinks. We believe that the orientation of wrinkles is based on the following mechanism. If the entire volume of PDMS elastomer shrinks homogeneously, the entire gold film will wrinkle (Figure 7b). However, by deforming as shown in Figure 7c, the compressive stress in the region near the edge is relieved. Therefore, the gold film does not wrinkle near the edges. Thus, when the distance between both edges of the sample is sufficiently short, no wrinkles form, or wrinkles form in only a small region limited to the center of the sample (Figure 7c). In contrast, when the distance is long, wrinkles form, as depicted in Figure 7d. Therefore, when a narrow and long strip of PDMS is used (see Figure 7e), wrinkles oriented form in the direction parallel to the *x*-axis because the distance between both edges of interest is long. However, wrinkles parallel to the *y*-axis do not form because, in this case, the distance between both edges of interest is short. As a result, only wrinkles parallel to the *x*-axis are observed. Although this is a qualitative explanation of the mechanism of the orientation of the wrinkles, Bowden *et al.* expressed the mechanism in more theoretical terms.[37]

Formation of wrinkles with IDA pattern
In order to obtain wrinkles with an IDA pattern, we planned to create an arrangement where an array of wrinkles with wavelength λ was put between two other arrays of wrinkles with wavelength 2λ, as shown in Figure 8. As described in the previous section, such an array of wrinkles can be easily obtained using narrow and long PDMS samples. In addition, the wavelength can be controlled by simply changing the thickness of the gold film.

The experimental procedure is briefly summarized as follows (see Figure 1). First, a gold film was deposited onto a PDMS strip typically
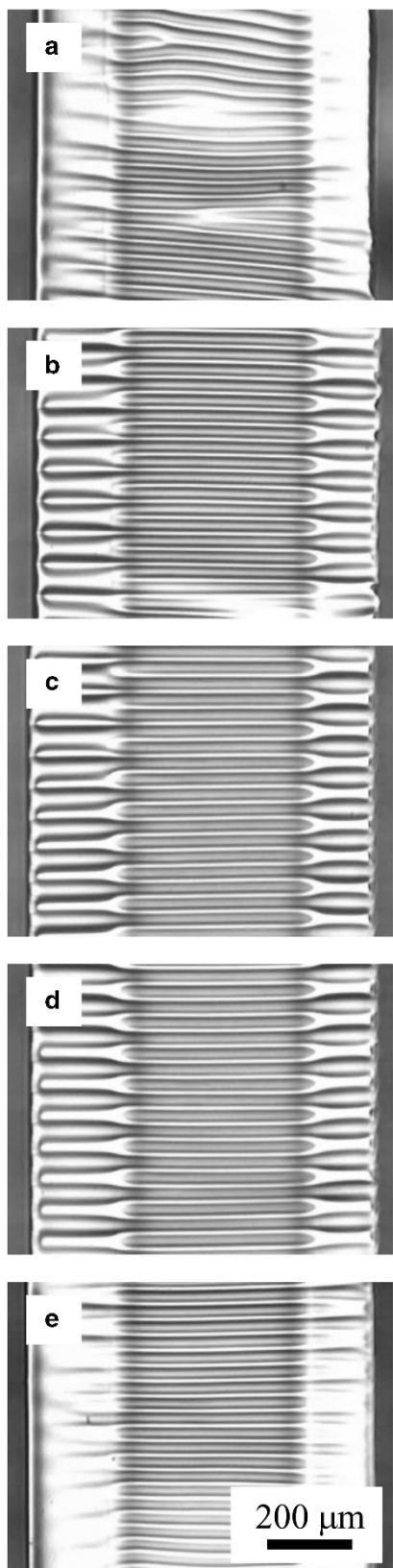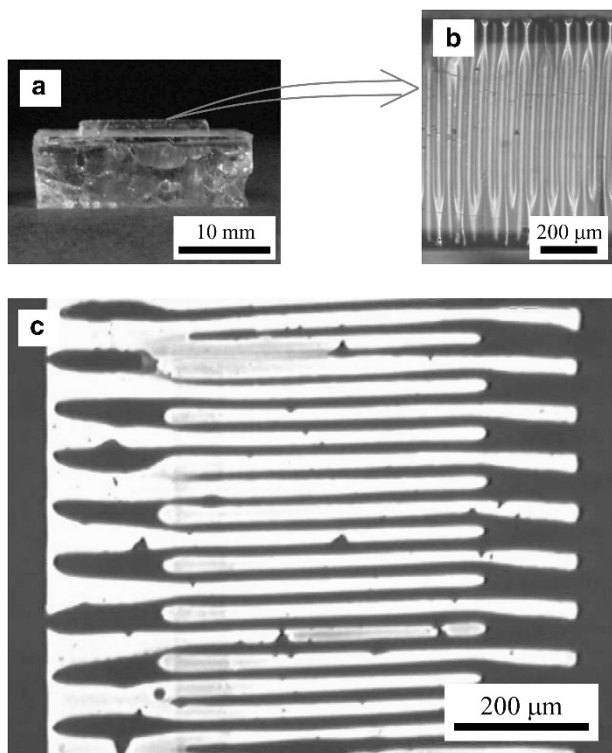
Figure 9 Light microscope images of gold film formed by repeating sputter deposition twice. The observation positions on the sample (**a**–**e**) were the same as those in the left diagram of Figure 3. A full color version of this figure is available at *Polymer Journal* online.
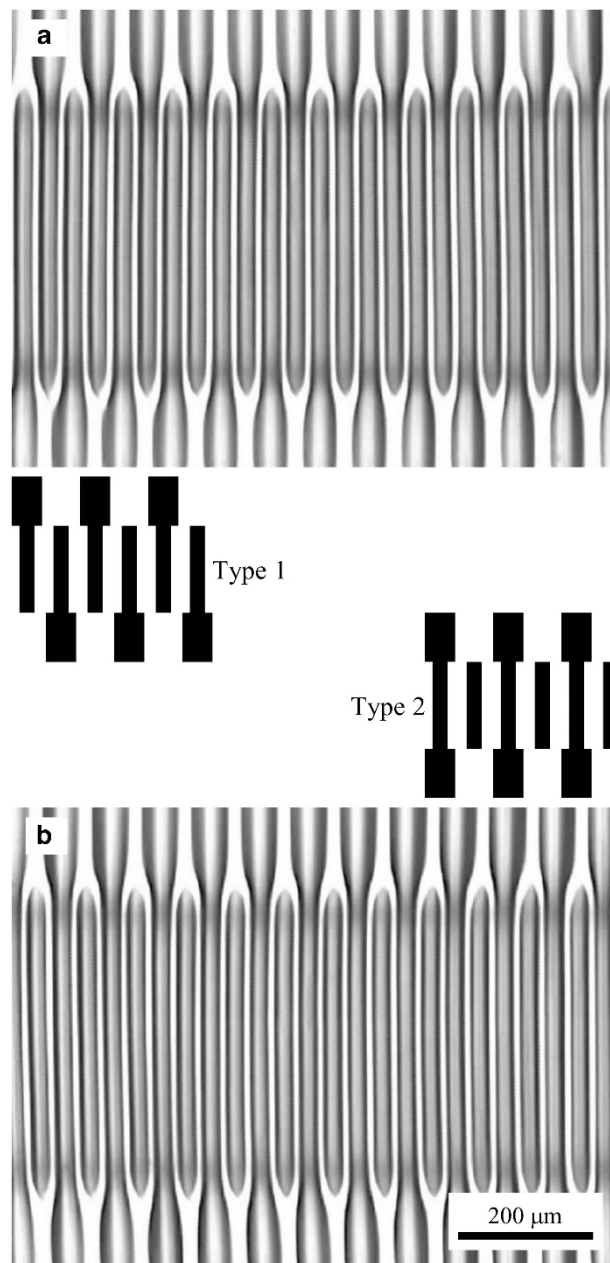
Figure 10 Light microscope images of gold films with well-ordered interdigitated array patterns. The patterns had (**a**) glide symmetry and (**b**) line symmetry. A full color version of this figure is available at *Polymer Journal* online.

0.85 mm wide. By this deposition, an array of winkles (wavelength $= \lambda$) was formed (Figure 1a). A glass strip 0.5-mm wide, which was used as a mask during the sputter deposition, was then placed on the PDMS strip (Figure 1b). The glass strip was slightly lifted above the PDMS strip so as not to damage the gold film formed by the previous deposition. Finally, gold deposition was performed again to create the side arrays of wrinkles whose wavelength was 2λ (Figure 1c).

Figure 9 shows an example of the wrinkles obtained using the above-mentioned procedure. The first deposition was conducted for 35 min and the second one was for 57.5 min. Although we could not obtain wrinkles with a perfectly IDA pattern over the entire surface of

Figure 11 (a) Photograph of stamp obtained by replicating the wrinkled gold film. (b) Light microscope images of stamp surface. (c) Light microscope image of gold coating on glass slide patterned using microcontact printing technique. A full color version of this figure is available at Polymer Journal online.

the sample, well-ordered patterns (that is, defect-free IDA patterns) were observed in some limited areas (Figure 10). Although reproducibility of such a well-ordered pattern was also not very high, we could achieve it 19 times by repeating the experiment 54 times.

The thickness of gold film in the center part (see Figure 8) was 63 nm ($= 1.8$ nm min$^{-1} \times 35$ min). That in the side part was 166.5 nm ($= 1.8$ nm min$^{-1} \times (35+57.5)$ min). Thus, the ratio of film thickness of the center part to that of the side part was 1:2.6. Because the wrinkle wavelength was proportional to the thickness of the gold film (Figure 6e) and the intended ratio of the wavelength of the center part to the side part was 1:2 (Figure 8), the best ratio of the film thickness would theoretically be concluded to be 1:2. However, the experimentally optimized ratio was 1:2.6. This discrepancy might be attributed to the fact that the second deposition was carried out onto an already wrinkled gold film, not onto a flat film.

The obtained IDA pattern included two types, type 1 and type 2 (see the schematic diagrams in Figure 10). Type 1 had glide symmetry, whereas type 2 had line symmetry. Type 1 was more frequently observed than was type 2, implying that type 1 might be more stable than type 2. However, the reason for this result has not yet been sufficiently clarified. Further investigation is necessary from the perspective of mechanics of materials.

Transfer of the IDA pattern of the wrinkles to a glass slide using microcontact printing techniques

As described in the introduction, we have intended to utilize the wrinkles with iIDA pattern for producing IDA microelectrodes. In

order to transfer the pattern to a glass slide, we used a technique called microcontact printing where a stamp made from PDMS and self-assembled monolayers (SAMs) of alkanethiols were employed.[36]

First, a replica of the wrinkled gold film was fabricated by casting a liquid precursor of PDMS elastomer on the wrinkled film (Figure 2a), followed by vulcanizing it. Because the obtained replica (Figure 2b) was a negative one, replication was repeated again using the negative replica as a mold. During this replication step, the gold film transferred from the negative replica to the positive one, as depicted in Figure 2c. The transferred gold film was then removed using wet etching (Figure 2d).[57] The obtained replica (Figures 11a and b) was used as a stamp in the next step.

The height of the surface at the center part of the stamp did not seem to be much different from that at the side part, based on the light microscope image where both parts were in clear focus (Figure 10; normal light microscopes are known to have shallow depths of focus). In addition, because the stamp was made from PDMS, which is a compliant, elastic material, such a small difference in height would not affect the stamped pattern very much.

The stamp that had preabsorbed 1-eicosanethiol was brought into contact with a glass slide coated with gold to form a SAM of 1-eicosanethiol with an IDA pattern. By means of wet etching to remove the gold coating outside the area patterned by SAM,[57] an IDA pattern appeared on the glass slide (Figure 11c).

Unfortunately, the patterned gold coatings were often peeled off during the rinsing step with water after the etching. This problem might result from the lack of an adhesion layer between the coating and the glass slide. Although an adhesion layer, which is normally obtained by depositing titanium or chromium, is used in a typical patterning protocol,[36] any equipment to prepare such an adhesion layer was unfortunately not available to us.

CONCLUSION
We have shown that an IDA pattern can spontaneously form on a wrinkled gold film deposited on a PDMS strip. Such a relatively complex pattern is obtained by using a gold film having different thicknesses. That is, the gold film on the PDMS strip is divided into three sections: the center section and two side sections. The thickness in the side sections is thicker than that in the center section. By optimizing the ratio between these thicknesses, wrinkles with an IDA pattern are obtained. In addition, the pattern of wrinkles can be transferred to a gold coating on a glass slide by means of microcontact printing techniques. Such a patterned gold coating is potentially useful as IDA microelectrodes for chemical and biochemical sensors.

ACKNOWLEDGEMENTS

1 White, R. M. & Voltmer, F. W. Direct piezoelectric coupling to surface elastic waves. Appl. Phys. Lett. 7, 314–316 (1965).
2 Sanderson, D. G. & Anderson, L. B. Filar electrodes: steady-state currents and spectroelectrochemistry at twin interdigitated electrodes. Anal. Chem. 57, 2388–2393 (1985).
3 Kim, S. K., Hesketh, P. J., Li, C., Thomas, J. H., Halsall, H. B. & Heineman, W. R. Fabrication of comb interdigitated electrodes array (IDA) for a microbead-based electrochemical assay system. Biosens. Bioelectron. 20, 887–894 (2004).
4 Varshney, M. & Li, Y. Interdigitated array microelectrodes based impedance biosensors for detection of bacterial cells. Biosens. Bioelectron. 24, 2951–2960 (2009).
5 Lange, K., Rapp, B. E. & Rapp, M. Surface acoustic wave biosensors: a review. Anal. Bioanal. Chem. 391, 1509–1519 (2008).

6 Zaccheo, B. A. & Crooks, R. M. Detection of an Epstein-Barr genome analog at physiological concentrations via the biometallization of interdigitated array electrodes. *Anal. Chem.* **81**, 5757–5761 (2009).

7 Ino, K., Kitagawa, Y., Watanabe, T., Shiku, H., Koide, M., Itayama, T., Yasukawa, T. & Matsue, T. Detection of hormone active chemicals using genetically engineered yeast cells and microfluidic devices with interdigitated array electrodes. *Electrophoresis* **30**, 3406–3412 (2009).

8 Tom-Moy, M., Baer, R. L., Spira-Solomon, D. & Doherty, T. P. Atrazine measurements using surface transverse wave devices. *Anal. Chem.* **67**, 1510–1516 (1995).

9 Du, Z., Li, C., Li, L., Yu, H., Wang, Y. & Wang, T. Ammonia gas detection based on polyaniline nanofibers coated on interdigitated array electrodes. *J. Mater. Sci.-Mater. Electron* **22**, 418–421 (2011).

10 Tomcik, P., Jencusova, P., Krajcikova, M., Bustin, D. & Brescher, R. The detection of formaldehyde in textiles using interdigitated microelectrode array diffusion layer titration with electrogenerated hypobromite. *Anal. Bioanal. Chem.* **383**, 864–868 (2005).

11 Ho, K.-C. & Liao, J.-Y. NO_2 gas sensing based on vacuum-deposited TTF-TCNQ thin films. *Sens. Actuator B Chem.* **93**, 370–378 (2003).

12 Jeong, J. W., Huh, J. W., Lee, J. I., Chu, H. Y., Pak, J. J. & Ju, B. K. Interdigitated electrode geometry effects on the performance of organic photoconductors for optical sensor applications. *Thin Solid Films* **518**, 6343–6347 (2010).

13 Molina-Lopez, F., Briand, D. & de Rooij, N. F. All additive inkjet printed humidity sensors on plastic substrate. *Sens. Actuator B Chem.* **166–167**, 212–222 (2012).

14 Morgan D. P. *Surface-Wave Devices for Signal Processing.* Amsterdam: Elsevier, 1985.

15 Kurosawa, M. K. State-of-the-art surface acoustic wave liner motor and its future applications. *Ultrasonics* **38**, 15–19 (2000).

16 Tang, W. C., Nguyen, T. H., Judy, M. W. & Howe, R. T. Electrostatic-comb drive of lateral polysilicon resonators. *Sens. Actuator A Phys.* **A21–A23**, 328–331 (1990).

17 Jo, M. C. & Guldiken, R. Dual surface acoustic wave-based active mixing in a microfluidic channel. *Sens. Actuator A Phys.* **196**, 1–7 (2013).

18 Zhang, A. & Zha, Y. Rapid drop-to-drop liquid-liquid microextraction by help of surface acoustic wave. *Chem. Eng. Process.* **62**, 145–149 (2012).

19 Zhang, A., Wei, Y. & Han, Q. A microreactor with surface acoustic wave micro-heating system. *Ferroelectrics* **432**, 22–31 (2012).

20 Guttenberg, Z., Muller, H., Habermuller, H., Geisbauer, A., Pipper, J., Felbel, J., Kielpinski, M., Scriba, J. & Wixforth, A. Planar chip device for PCR and hybridization with surface acoustic wave pump. *Lab Chip* **5**, 308–317 (2005).

21 Yasukawa, T., Hatanaka, H. & Mizutani, F. Simple detection of surface antigens on living cells by applying distinct cell positioning with negative dielectrophoresis. *Anal. Chem.* **84**, 8830–8836 (2012).

22 Yamamoto, M., Yasukawa, T., Suzuki, M., Kosuge, S., Shiku, H., Matsue, T. & Mizutani, F. Patterning with particles using three-dimensional interdigitated array electrodes with negative dielectrophoresis and its application to simple immunosensing. *Electrochim. Acta* **82**, 35–42 (2012).

23 Chen, Y., Ding, X., Lin, S. S., Yang, S., Huang, P., Nama, N., Zhao, Y., Nawaz, A. A., Guo, F., Wang, W., Gu, Y., Mallouk, T. E. & Huang, T. J. Tunable nanowire patterning using standing surface acoustic waves. *ACS Nano* **7**, 3306–3314 (2013).

24 Strobl, C. J., Schaflein, C., Beierlein, U., Ebbecke, J. & Wixforth, A. Carbon nanotube alignment by surface acoustic waves. *Appl. Phys. Lett.* **85**, 1427–1429 (2004).

25 Belmont, C. & Girault, H. H. Coplanar interdigitated band electrodes for electrosynthesis part II: methoxylation of furan. *J. Appl. Electrochem.* **24**, 719–724 (1994).

26 Berggren, C., Bjarnason, B. & Johansson, G. Capacitive biosensors. *Electroanalysis* **13**, 173–180 (2001).

27 Niwa, O. Electroanalysis with interdigitated array microelectrodes. *Electroanalysis* **7**, 606–613 (1995).

28 Takahashi, M., Morita, M., Niwa, O. & Tabei, H. Highly sensitive high-performance liquid chromatography detection of catecholamine with interdigitated array microelectrodes. *J. Electroanal. Chem.* **335**, 253–263 (1992).

29 Sielmann, C. J., Busch, J. R., Stoeber, B. & Walus, K. Inkjet printed all-polymer flexural plate wave sensors. *IEEE Sens. J.* **13**, 4005–4013 (2013).

30 Daniel, D. & Gutz, I. G. R. Quick production of gold electrode sets or arrays and of microfluidic flow cells based on heat transfer of laser printed toner masks onto compact discs. *Electrochem. Commun.* **5**, 782–786 (2003).

31 Ho, W. O., Krause, S., McNeil, C. J., Pritchard, J. A., Armstrong, R. D., Athey, D. & Rawson, K. Electrochemical sensor for measurement of urea and creatinine in serum based on ac impedance measurement of enzyme-catalyzed polymer transformation. *Anal. Chem.* **71**, 1940–1946 (1999).

32 Loo, Y.-L., Willett, R. L., Baldwin, K. W. & Rogers, J. A. Additive, nanoscale patterning of metal films with a stamp and a surface chemistry mediated transfer process: applications in plastic electronics. *Appl. Phys. Lett.* **81**, 562–564 (2002).

33 Ahn, B. Y., Duoss, E. B., Motala, M. J., Guo, X., Park, S.-I., Xiong, Y., Yoon, J., Nuzzo, R. G., Rogers, J. A. & Lewis, J. A. Omnidirectional printing of flexible, stretchable, and spanning silver microelectrodes. *Science* **323**, 1590–1593 (2009).

34 Parashkov, R., Becker, E., Riedl, T., Johannes, H.-H. & Kowalsky, W. Large area electronics using printing methods. *Proc. IEEE* **93**, 1321–1329 (2005).

35 Chung, J. Y., Nolte, A. J. & Stafford, C. M. Surface wrinkling: a versatile platform for measuring thin-film properties. *Adv. Mater.* **23**, 349–368 (2011).

36 Qin, D., Xia, Y. & Whitesides, G. M. Soft lithography for micro- and nanoscale patterning. *Nat. Protoc.* **5**, 491–502 (2010).

37 Bowden, N., Brittain, S., Evans, A. G., Hutchinson, J. W. & Whitesides, G. M. Spontaneous formation of ordered structures in thin films of metals supported on an elastomeric polymer. *Nature* **393**, 146–149 (1998).

38 Watanabe, M. Striped-pattern formation of a thin gold film deposited onto a stretched elastic silicone substrate. *J. Polym. Sci. Pt. B Polym. Phys.* **43**, 1532–1537 (2005).

39 Ohzono, T. & Shimomura, M. Ordering of microwrinkle patterns by compressive strain. *Phys. Rev. B* **69**, 132202 (2004).

40 Yoo, P. J., Suh, K. Y., Park, Y. & Lee, H. H. Physical self-assembly of microstructures by anisotropic buckling. *Adv. Mater.* **14**, 1383–1387 (2002).

41 Lin, P.-C. & Yang, S. Spontaneous formation of one-dimensional ripples in transit to highly ordered two-dimensional herringbone structures through sequential and unequal biaxial mechanical stretching. *Appl. Phys. Lett.* **90**, 241903 (2007).

42 Breid, D. & Crosby, A. J. Effect of stress state on wrinkle morphology. *Soft Matter* **7**, 4490–4496 (2011).

43 Watanabe, M. Wrinkles with a well-ordered checkerboard pattern, created using dip-coating of poly(methyl methacrylate) on a UV-ozone-treated poly(dimethylsiloxane) substrate. *Soft Matter* **8**, 1563–1569 (2012).

44 Shih, T.-K., Ho, J.-R., Chen, C.-F., Whang, W.-T. & Chen, C.-C. Topographic control on silicone surface using chemical oxidization method. *Appl. Surf. Sci.* **253**, 9381–9386 (2007).

45 Watanabe, M. & Mizukami, K. Well-ordered wrinkling patterns on chemically oxidized poly(dimethylsiloxane) surfaces. *Macromolecules* **45**, 7128–7134 (2012).

46 Watanabe, M. & Shinoda, K. Self-structured serrated edges of chemically oxidized poly (dimethylsiloxane) disks. *J. Appl. Polym. Sci.* **131**, 40767 (2014).

47 Watanabe, M. & Hashimoto, R. Area-selective micro-wrinkle formation on poly (dimethylsiloxane) by treatment with strong acid. *J. Polym. Sci. Pt. B Polym. Phys* (e-pub ahead of print 25 September 2014; doi:10.1002/polb23599).

48 Efimenko, K., Rackaitis, M., Manias, E., Vaziri, A., Mahadevan, L. & Genzer, J. Nested self-similar wrinkling patterns in skins. *Nat. Mater.* **4**, 293–297 (2005).

49 Sultan, E. & Boudaoud, A. The buckling of a swollen thin gel layer bound to a compliant substrate. *J. Appl. Mech.* **75**, 051002 (2008).

50 Chen, X. & Hutchinson, J. W. Herringbone buckling patterns of compressed thin films on compliant substrates. *J. Appl. Mech.* **71**, 597–603 (2004).

51 Chung, J. Y., Nolte, A. J. & Stafford, C. M. Diffusion-controlled, self-organized growth of symmetric wrinkling patterns. *Adv. Mater.* **21**, 1358–1362 (2009).

52 Hyun, D. C., Moon, G. D., Park, C. J., Kim, B. S., Xia, Y. & Jeong, U. Buckling-assisted patterning of multiple polymers. *Adv. Mater.* **22**, 2642–2646 (2010).

53 Ionescu, R. E., Fillit, C., Jaffrezic-Renault, N. & Cosnier, S. Urease-gelatin interdigitated microelectrodes for the conductometric determination of protease activity. *Biosens. Bioelectron.* **24**, 489–492 (2008).

54 Son, S. U., Seo, J.-H., Choi, Y. H. & Lee, S. S. Fabrication of a disposable biochip for measuring percent hemoglobin A1c. *Sens. Actuator A Phys* **130–131**, 267–272 (2006).

55 Chikae, M., Idegami, K., Kerman, K., Nagatani, N., Ishikawa, M., Takamura, Y. & Tamiya, E. Direct fabrication of catalytic metal nanoparticles onto the surface of a screen-printed carbon electrode. *Electrochem. Commun.* **8**, 1375–1380 (2006).

56 Shim, J. S., Rust, M. J. & Ahn, C. H. A large area nano-gap interdigitated electrode array on a polymer substrate as a disposable nano-biosensor. *J. Micromech. Microeng* **23**, 035002 (2013).

57 Saalmink, M., van der Marel, C., Stapert, H. R. & Burdinski, D. Positive microcontact printing with mercaptoalkyloligo(ethylene glycol)s. *Langmuir* **22**, 1016–1026 (2006).

58 Cerda, E. & Mahadevan, L. Geometry and physics of wrinkling. *Phys. Rev. Lett.* **90**, 074302 (2003).

59 Kagaku-binran Kiso-hen Kaitei-5th edn (ed. The Chemical Society of Japan) (Maruzen, Tokyo, Japan, 2004) in Japanese.

60 Casper, M. D., Gozen, A. O., Dickey, M. D., Genzer, J. & Maria, J.-P. Surface wrinkling by chemical modification of poly(dimethylsiloxane)-based networks during sputtering. *Soft Matter* **9**, 7797–7803 (2013).